

Sensing Tactile Microvibrations with the BioTac – Comparison with Human Sensitivity

Jeremy A. Fishel, *Student Member*, and Gerald E. Loeb, *Senior Member*

Abstract— The human fingertip is exquisitely sensitive to vibrations that are essential to detect slip and discriminate textures. Achieving similar functions with prosthetic and robotic hands will require tactile sensors with similar sensitivity. Many technologies have been developed to sense such vibrations, yet none have achieved the requisite sensitivity in a package that is robust enough to meet practical applications. The BioTac®, developed by the authors, uses an incompressible liquid as an acoustic conductor to convey vibrations from the skin to a wide bandwidth pressure transducer located deep in the rigid core of the mechatronic finger, where it is protected from damage. Signal conditioning electronics were designed to achieve sensitivity down to the theoretical noise floor of the transducer, making the device very sensitive to the smallest of vibrations, even sound. We demonstrate here that this device exceeds human performance in detecting sustained vibrations (capable of sensing vibrations as small as a few nanometers at ~330Hz) as well as very small transient events that arise when small particles are dropped on the finger. This overcomes the supposition that such sensitivity requires fragile sensory elements to reside near the vulnerable contact surfaces.

I. INTRODUCTION

HUMANS have exquisite sensitivity to mechanical vibrations in the skin. Pacinian corpuscles with frequency responses of 60-700Hz [1] are capable of measuring vibrations associated with slip that can be less than a micrometer around their center frequency of 200 Hz [2][3]. The sensitivity to such vibrations plays an integral role in many important tasks such as slip detection for the control of grip [4-6] and the perception of fine textures[7-9]. It has been demonstrated that eliminating tactile sensitivity with nerve block renders the human hand almost useless in even the simplest of tasks [10]. Artificial systems seeking to obtain these capabilities will require tactile sensors with performance similar to that found in the human finger; otherwise they are likely to be severely limited, similarly to the anesthetized human hand.

Development of artificial tactile sensors is not new and there are many reviews that cover their evolution over the years [11-14]. Most of the attention has focused specifically

Manuscript received January 31, 2012. This work concerns a technology being developed commercially by SynTouch, LLC where both authors are principals. This work was supported in part by the Eunice Kennedy Shriver National Institute of Child Health & Human Development of the National Institutes of Health Grant 5R44HD061165-03.

J. A. Fishel is with the University of Southern California, Los Angeles, CA and SynTouch, LLC, Los Angeles, CA (phone: 562-704-0786; e-mail: jeremyfishel@gmail.com).

G. E. Loeb, is with the University of Southern California, Los Angeles CA, and SynTouch, LLC, Los Angeles, CA (e-mail: geloeb@gmail.com).

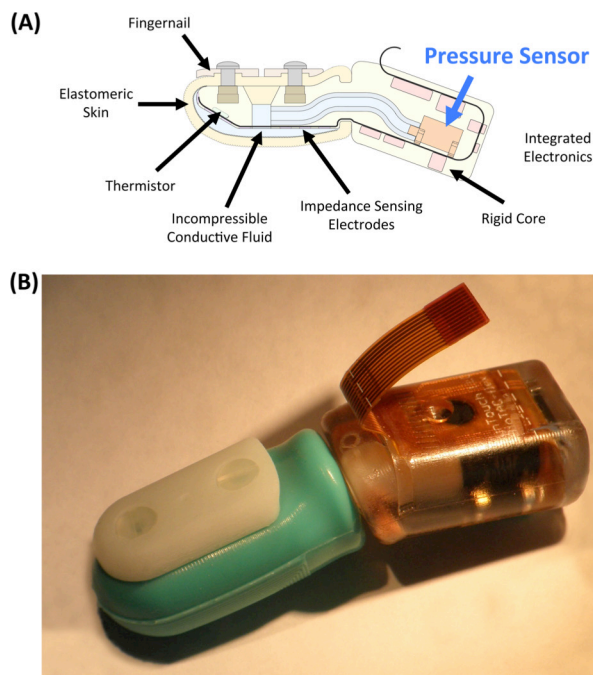


Fig. 1. A) Cross-sectional schematic of the BioTac. B) Photograph of an assembled BioTac. Fingerprint-like ridges can be seen on the ventral surface.

on the sensing of high-resolution normal forces, which only represents a small subset of human touch. Human fingertips are also sensitive to shear forces and skin stretch, temperature and thermal fluxes, as well as vibration. Such multimodal sensitivity is necessary to achieve the dexterity and performance of the human hand [15].

Developing a tactile sensor with similar form and function as the human finger presents a unique design challenge, particularly for the sensing of vibrations. The sensor must be sensitive enough to detect vibrations smaller than a micrometer yet robust enough to deform a few millimeters without damage. Many groups have explored dynamic tactile sensing with a variety of sensory technologies such as accelerometers [16], piezoelectric polymers [17-20], magneto-inductance [21], and ultrasonic technologies [22], [23]. While these sensors work fine for specific applications in controlled laboratory environments, they all share the common trait of requiring fragile sensing mechanisms to reside near the contact surface of the sensor. Some developers have even concluded that this was a requirement for such sensory capabilities [12]. Both mechatronic and human fingers are frequently exposed to conditions where

they can be damaged, but biological appendages possess the ability to regenerate damaged skin and tactile receptors therein. An alternative approach for engineered systems is to keep delicate sensing devices a safe distance from possible damage, while still retaining as much sensitivity as possible.

The BioTac (Fig. 1) was designed to meet this need for robustness and sensitivity. It consists of a rigid core that contains all sensory transducers, covered by an elastomeric skin. The space between the skin and the core is inflated with an incompressible and conductive fluid to give it a compliance that mimics human fingerpads. No sensory transducers or wires are contained in the skin making the design robust to grit, moisture and physical damage to sensory mechanisms that typically plague other tactile sensors. If the skin of the BioTac becomes damaged or worn it can be easily replaced.

The BioTac consists of three complimentary sensory modalities (force, vibration and temperature) that have been integrated into a single package. Contact forces distort the elastic skin and underlying conductive fluid, changing impedances of electrodes distributed over the surface of the rigid core [24-26]. Vibrations in the skin propagate through the fluid and are detected as AC signals by the hydro-acoustic pressure sensor [27]. Temperature and heat flow are transduced by a thermistor near the surface of the rigid core [28]. This paper describes the design and performance of the vibration sensing modality of the BioTac.

II. METHODS

A. Physics of Fluidic Vibration Sensing

Preliminary studies demonstrated the feasibility of sensing slip-related microvibrations in a liquid-filled fingertip by measuring the dynamic pressure of the liquid [27]. The incompressibility of the liquid and long wavelengths at the frequencies of interest ($\lambda = 3\text{m}$ at 500Hz in water) allow for the sensing elements to be moved away from the contact region where it would be susceptible to damage. This permits for a class of highly robust and simple tactile vibration sensitivity that has been integrated into the multimodal sensory suite of the BioTac.

The tube that connects the liquid under the skin to the pressure transducer (i.e. hydrophone) in the core also has a resonant frequency (f), which can be calculated from the media's speed of sound (v) and the length of the tube (L) by the acoustic resonance formula of a closed tube:

$$f = v/4L \quad (1)$$

For a 2cm tube filled with saltwater ($v = 1497\text{m/s}$), this resonant frequency is 18.7kHz. The desired bandwidth to mimic biological performance is 1 kHz so the resonance of a 2cm tube is substantially high enough to be ignored. Another factor to consider is the inertial damping of the fluid. Increasing the length of the tube, viscosity or compressibility of the fluid increases the attenuation of pressure signals, particularly at higher frequencies. Using a low viscosity

liquid such as water and keeping the fluid tube as short as possible can mitigate these effects.

B. Fabrication of the BioTac

The BioTac core includes a flexible circuit that contains all of the sensory electronics, signal conditioning circuits and microcontroller [28]. The flexible circuit is loaded into a three-part mold and filled with an epoxy (Stycast 1264, Emerson & Cuming) to produce the core of the BioTac. Skins are molded from a silicone (Silastic S, Dow Corning) in a three-part mold that has features to mold artificial ridges similar to fingerprints. The fingernail is machined from acrylic. Once the parts are assembled (Fig. 1B) the BioTac is filled with a solution that minimizes changes in volume due to diffusion through the skin (82% Polyethylene Glycol and 18% distilled water that is mixed with NaBr to produce a 1M solution). Care is taken to ensure there are no bubbles inside the fingertip after filling with fluid. The salinity of this mixture provides the conductivity required for the impedance sensing modality of the BioTac [26]. This solution was indistinguishable from pure water with regard to the vibration sensing modality discussed in this paper.

C. Electronics Design and Noise Analysis

The BioTac contains all necessary electronics for signal conditioning, analog to digital conversion and serial transmission of data from all sensors. The signal conditioning electronics were redesigned to detect signals as close as possible the theoretical noise floor of the piezoresistive transducer.

1) Thermal Noise

Electronic noise arises in all conductors regardless of applied voltage because the charge carriers inside a conductor vibrate stochastically due to thermal energy. The root-mean-square (RMS) amplitude of the noise can be calculated from the Boltzmann constant (k_b), the temperature (T), the resistive load (R), and the bandwidth (Δf) from the following equation:

$$V_{thermal} = \sqrt{4 k_b T R \Delta f} \quad (2)$$

Thermal noise was minimized by low-pass analog filtering with a 1040Hz cutoff frequency and selecting a pressure transducer (Honeywell 24PC15SMT) with low output resistance. An alternative sensor (Honeywell 26PC15SMT) offered temperature compensation to reduce low-frequency drift with changing temperature but had a much larger output resistance and would have increased this noise source. The selected transducer operates as a piezoresistive bridge with an output resistance of 5k Ω (Fig. 2A). The BioTac is heated to about 35C for thermal flux measurements [28]. The thermal noise is thus 0.29 μVrms .

The output of the transducer in response to pressure is specified as 0.218mV/V \cdot kPa (1.5mV/V \cdot psi) and increases as the supply voltage to the bridge increases. Given that the thermal noise stays constant, a very simple trick to improve

the signal-to-noise ratio is to increase the supply voltage. While most electronics included in the BioTac are powered at 3.3V, we added a 10V regulated signal for the transducer. The output of the transducer with a 10V supply is 2.18mV/kPa (15mV/psi). The thermal noise of 0.29 μ V would then be the equivalent of 0.133Pa (0.0193 $\times 10^{-3}$ psi).

2) Signal Conditioning and Amplifier Noise

The transducer output is amplified with a gain of 10 and a low-pass anti-aliasing filter at 1040Hz to produce a DC pressure signal (Fig. 2B). A second stage with a band-pass filter of 10-1040Hz and an additional gain of 99.1 produces the high-resolution vibration signal (AC pressure). Both the DC and AC pressures are sampled by a microcontroller inside the BioTac with 12-bit resolution for the range 0-3.3V. This accommodates the full range of transducer output (103.4kPa = 15psi) with a resolution of 36.5Pa (5.3 $\times 10^{-3}$ psi) at the DC stage and ± 758 Pa (0.110psi) range with a 0.37Pa (0.054 $\times 10^{-3}$ psi) resolution at the AC stage.

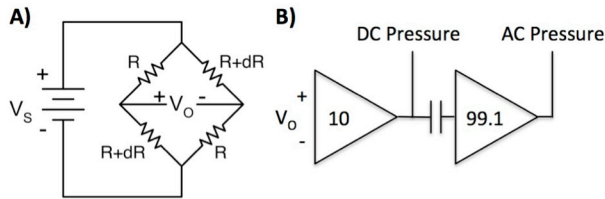


Fig. 2. A) Electrical schematic of the piezoresistive strain bridge used in the pressure transducer. The transducer includes two fixed resistors and two variable resistors that change in response to applied pressure. B) Conceptual diagram of amplifier circuit used to create DC pressure and AC pressure signals.

First stage amplifier noise tends to be a significant source of noise so a low-noise amplifier was selected (AD8624, Analog Devices). For 1024Hz bandwidth, it generates 0.39 μ V of voltage noise referred to input. The device also generates 4.8pA of current noise, but with a 5k Ω load this source is comparatively negligible ($\sim 0.025\mu$ V). The second stage amplifier has similar input noise, but the gain of 10 on the first stage amplifier makes the noise contribution of the second stage negligible when referred to input.

3) Capacitively Coupled Extrinsic Noise

Any extrinsic AC signal can contribute noise by capacitive coupling into the conductors comprising the measurement circuitry. One common source is the 60Hz electrical power lines. In our system the primary source of this noise is the high-speed digital communication lines operating at up to 10MHz. To reduce stray capacitance, care was taken to redesign the circuitry to shorten leads of low voltage un-amplified signals and move them away from digital communication lines. To further reduce interference, the microcontroller was configured to sample the analog inputs at times when the digital communication between the BioTac and the host was silent.

D. Total Noise Calculation and Validation

Computed noise is summarized in Table I. The total RMS noise of 0.49 μ V was computed as the root sum of squares of thermal and input noise. This does not include extrinsic

sources of noise such as stray capacitance or power supply noise. Based on the sensitivity of the transducer this amount of noise would be equivalent to 0.224Pa (0.033 $\times 10^{-3}$ psi) of pressure or 0.6 of the least-significant-bit (lsb) value of digitized AC pressure (the lsb value is hereafter referred to as “bits”).

TABLE I
SUMMARY OF THEORETICAL NOISE SOURCES

| Noise Source | RMS Noise | Notes |
|-----------------------|--------------|--------------------------------|
| Thermal Noise | 0.29 μ V | Inherent in transducer |
| Amplifier Input Noise | 0.39 μ V | Noise of first stage amplifier |
| Stray Capacitance | - | Not estimated. |
| Total Noise | 0.49 μ V | |

E. Data Acquisition

The BioTac uses SPI protocol for digital communication. A high-speed SPI/USB device (Cheetah, Total Phase) was used to command the BioTac to sample the AC and DC pressure signals at 2.2kS/s (kilosamples per second) each for a total of 4.4kS/s. Software (LabVIEW, National Instruments) was developed to communicate with the SPI controller and queue up batches of asynchronous sampling commands in 100ms blocks of data that were transferred to the host through USB as they became available at the controller. Data were saved to text files and analyzed offline in MATLAB (MathWorks).

F. Signal-to-Noise Estimation

Background RMS noise and signal power were calculated as the standard deviation and variance of the AC pressure signal when the BioTac was at rest and without any vibration disturbances. Signal-to-noise ratio was computed for common tasks with the BioTac: 1) sliding over a textured piece of foam, 2) making light taps, and 3) clicking on a computer mouse. The signals are presented as time plots.

G. Comparison with Human Performance

Psychophysical and physiological studies have explored the sensitivity of the human fingertip to vibrations [1][29], but they are not necessarily comparable to stimuli applicable to the BioTac. We measured the thresholds for detection of applied vibrations and small impacts in five normal human volunteers who gave their informed consent to participate in this study. We compared these to the detectability of the corresponding AC pressure signals as defined below.

1) Frequency Sensitivity

Many different devices exist to apply vibrations to human skin with technologies such as eccentric motors or inductive coils [30], but their output amplitudes are often sensitive to mechanical load. We used a piezoelectric actuator (AE0203D16F, NEC/TOKIN) that produces 0.113 μ m/V of applied voltage with a 17.4 μ m displacement for maximal applied drive of 150V. The device had a high blocking force of 200N, making it stiff enough to be insensitive to the range of loads presented by the BioTac or human finger. Sinusoidal signals were generated by a function generator

and amplified by a commercial driver for piezoelectric devices (Piezomaster VP7206-24L105, Viking Industrial Products). The input to the actuator was monitored on an oscilloscope to confirm the frequency and amplitude.

To determine frequency sensitivity of the biological finger, subjects were asked to place their finger on the device with any force they chose and amplitude was varied over a set number of frequencies between 10 and 900Hz. At each frequency test, vibration amplitudes were increased from below the perceptual limits until subjects first reported the vibration sensation. All trials were repeated 3 times at each frequency and the mean value was determined. Thresholds determined in this manner were consistent among the repeat trials and similar among subjects, so more systematic methods such as Bekesy tracking were not employed. The average amplitudes at threshold of detectability and the performance of the most sensitive subjects are reported here.

To test frequency sensitivity of the BioTac, a 1 μ m drive signal was used at frequencies between 10 and 900Hz. The AC pressure signals were analyzed in the frequency domain with a 1s window. The frequency of maximum power was found to coincide with the drive stimulus frequency in all tests. Total signal power was calculated from the total energy in a 2Hz band centered on this peak frequency. The RMS value of AC pressure (square root of total power) was found to vary proportionally with applied vibration amplitude at all frequencies, confirming the linearity of vibration amplitude to sensed vibrations in the system. This linearity made it possible to determine the theoretical sensitivity at different frequencies based on the power estimated from a 1 μ m vibration. The background noise power with no vibration applied in the largest 2Hz band was found to be 0.2bits². The lowest detectable vibration amplitude was calculated as the point when the signal power was double the this background signal power using the following formula:

$$d_{\min} = 1\mu\text{m} \times \sqrt{\frac{0.4\text{bits}^2}{P_{1\mu\text{m}}}} \quad (3)$$

This equation was tested at multiple frequencies, including the peak sensitivity, and was found to be accurate in all cases.

2) Impact Sensitivity

To determine the sensitivity to impact, small spheres of various sizes and densities were dropped on either the BioTac or the human fingertip from a height of 7 cm through a guide hole drilled in a block of acrylic. Both the mass of the ball and impact energy (estimated from potential energy before the drop) were calculated. Six different sized spheres were used as outlined in Table II. It was observed that sensitivity scaled with impact energy rather than mass as smaller masses were readily detected from larger drop heights while they were difficult to detect at shorter ones.

TABLE II
SPHERES USED FOR IMPACT TESTS

| Sphere | Mass (mg) | Energy (μ J) |
|--------------------------|-----------|-------------------|
| 0.25 mm Solder Ball | 0.072 | 0.049 |
| 0.45 mm Solder Ball | 0.422 | 0.289 |
| 1 mm Aluminum Bearing | 1.461 | 1.002 |
| 1 mm Steel Bearing | 4.089 | 2.805 |
| 3/64 in Steel Bearing | 6.902 | 4.734 |
| 5/64 in Aluminum Bearing | 11.415 | 7.830 |

For assessment of human performance, subjects were asked to close their eyes while holding their finger under the guide hole and report when they felt any impacts. Five or more trials were completed for all spheres except for some of the larger spheres when it was quite obvious that the subject had no difficulty identifying the impacts. Results are presented as percentage of correct identifications averaged across all subjects.

To assess the sensitivity of the BioTac we used an algorithm to count the number of points that deviated past four standard deviations of noise. A confirmed detection of impact was classified as any event that produced more than 3 points outside of this range within a 100ms window. At a sampling rate of 2200S/s the likelihood of false positives in the 100ms window was 0.00027% (once every 10 hours) and was never observed when the BioTac was at rest.

III. RESULTS

A. Vibration Signals During Common Tasks

The BioTac was found to be highly sensitive to vibrations and transient signals during common tasks (Fig. 3). Background noise for vibration signal had an RMS value of approximately 1.4bits. Sliding over a foam texture therefore had a signal to noise ratio of greater than 1000. Signals such as the click and release of a mouse button were readily observable. The BioTac was even found to demonstrate such sensitivity that when resting on a table it could easily detect vibrations from a person walking by as well as loud acoustic emissions such as shouting.

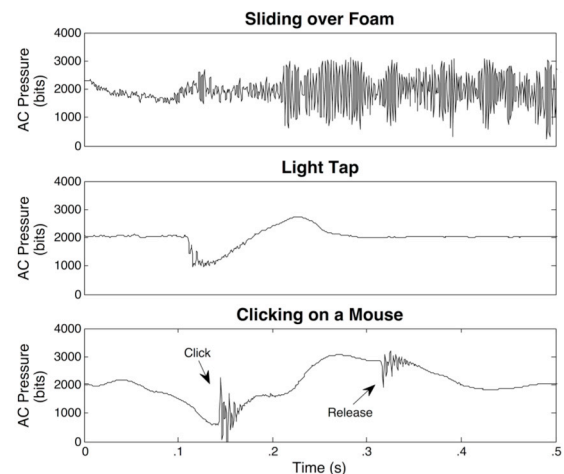


Fig. 3. BioTac vibration signals during common tasks. Background noise is approximately 1.4bits.

B. Theoretical vs. Actual Noise

Actual RMS noise of the AC pressure signal was verified to be 1.4 ± 0.1 bits, which is slightly more than double the theoretical noise of 0.6 bits based on the conservative analysis. Much of this noise is likely due to quantization noise of the analog-to-digital conversion itself. This 1.4 bits of noise corresponds to 0.52 Pa ($0.078 \times 10^{-3} \text{ psi}$) in terms of transducer noise.

C. Comparison with Human Performance

1) Frequency Sensitivity

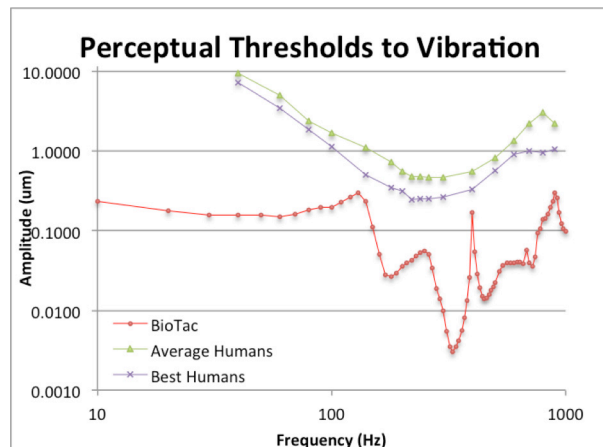


Fig. 4. Frequency Sensitivity Plots. Green trace = average subject performance; purple trace = best subject performance; red trace = BioTac sensitivity.

Plots comparing amplitudes of human sensitivity to BioTac sensitivity as a function of frequency are shown in Fig. 4. The BioTac had a rather complex transfer function that varied slightly with inflation volume and the location of the vibrational stimuli. For all frequencies and conditions, however, the sensitivity of the BioTac was better than the human subjects.

2) Impact Sensitivity

TABLE III
SUMMARY OF PERFORMANCE FOR IMPACT TESTS

| Sphere | Energy (μJ) | Human Classification | BioTac Classification |
|-----------------------|-------------|----------------------|-----------------------|
| 0.25mm Solder Ball | 0.049 | 0% | 0% |
| 0.45mm Solder Ball | 0.289 | 47.5% | 100% |
| 1mm Aluminum Bearing | 1.002 | 74.86% | 100% |
| 1mm Steel Bearing | 2.805 | 100% | 100% |
| 3/64in Steel Bearing | 4.734 | 100% | 100% |
| 5/64 Aluminum Bearing | 7.830 | 100% | 100% |

Table III compares human to BioTac sensitivity for correctly identifying the impact of various spheres. The BioTac was able to readily detect contact of all spheres except the smallest (0.25mm Solder Ball). Humans had a great deal of variation in performance with some subjects unable to detect reliably even the 1mm Aluminum Bearing (1.461mg). In most cases subjects were occasionally able to detect the 0.45 Solder Ball (0.422 mg) and only one subject was able to detect these every time; the BioTac had a 100% classification rate for the same object. Signals from the

BioTac (Fig. 5) resemble decaying sinusoids with a resonant frequency around 330Hz and a time constant of 20ms.

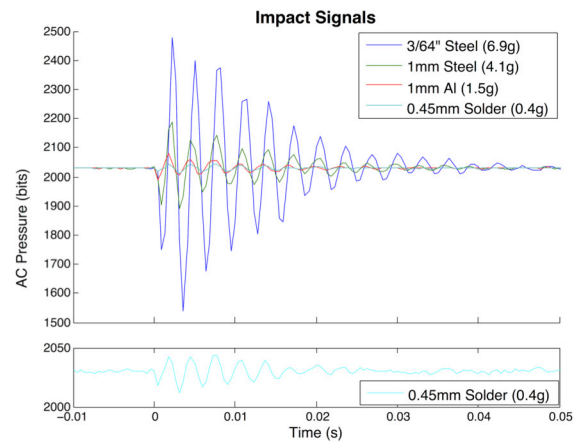


Fig. 5. Example signals of impact tests as detected in the BioTac. Lower plot is zoomed in on the y-axis to show background noise for impact sensitivity on the 0.45mm solder ball which was the lowest detectable stimuli tested.

IV. DISCUSSION

The vibration transmission and transduction system of the BioTac was found to be operating near the theoretical sensitivity of the transducer and signal conditioning system. Its sensitivity exceeded that of human fingertips for the full range of sinusoidal frequencies for which humans have tactile receptors and for impacts of tiny, low-mass objects. This contradicts previous claims [12] that such sensitivity to vibrations would require transducers near the contact surface, where they would be vulnerable to damage during normal use.

Compared to the strain-gage pressure transducer in the BioTac, piezoelectric transducers are known to have far superior signal-to-noise performance and would likely produce even better sensitivity when coupled with transmission of vibrations from skin through an incompressible fluid. They have two major drawbacks in this application, however: 1) they are not suitable for determining resting fluid pressure, and 2) they generally require more complex signal processing electronics.

The effects of silicone skin thickness and hardness on vibration sensitivity of the BioTac were examined anecdotally in preliminary research and were found to be relatively minor.

A. Future Work

The BioTac was designed to be biomimetic, a strategy that assumes that sensing capabilities at least similar to those of humans would be necessary for mechatronic systems to achieve humanlike haptic performance. Preliminary studies have demonstrated that the BioTac does actually generate rich patterns of vibrations as it contacts and slides over surfaces, but these patterns depend on the force and velocity of the exploratory movements that are applied to those

surfaces [27]. Thus much work is still required to develop algorithms to control such movements and to interpret the robust but complex sensory signals that the BioTac generates. Because these signals are similar in modalities, sensitivity and dynamic range to those from human fingertips, it should be possible to use biomimetic design to develop such algorithms. Given such algorithms, it should be possible for robots to achieve humanlike capabilities to discriminate and identify textures, detect slip, estimate coefficient of friction and adjust stability of grip.

ACKNOWLEDGMENTS

The authors would like to thank Gary Lin for the layout and design of the flexible circuit and support for electronics, Raymond Peck for the fabrication of the BioTac sensors used in these tests and Tomonori Yamamoto for his feedback and help. The authors would also like to thank the entire team at SynTouch, in addition to those already named, (Matthew Borzage, Nicholas Wettels, and David Groves) for their assistance on this project and teamwork. Also, many thanks to the Medical Device and Development Facility at the University of Southern California for their ongoing advice and feedback. Jeremy Fishel would like to thank Emily Ragsdale for all of the support and encouragement throughout this project.

REFERENCES

- [1] V. B. Mountcastle, R. H. LaMotte, and G. Carli, "Detection Thresholds for Stimuli in Humans and Monkeys: Comparison With Threshold Events in Mechanoreceptive Afferent Nerve Fibers Innervating the Monkey Hand," *Journal of Neurophysiology*, vol. 35, pp. 122–136, 1972.
- [2] G. Westling and R. S. Johansson, "Responses in Glabrous Skin Mechanoreceptors During Precision Grip in Humans," *Experimental Brain Research*, vol. 66, pp. 128–140, 1987.
- [3] A. J. Brisben, S. S. Hsiao, and K. O. Johnson, "Detection of Vibration Transmitted Through an Object Grasped in the Hand," *Journal of Neurophysiology*, vol. 81, pp. 1548–1558, 1999.
- [4] R. S. Johansson and G. Westling, "Signals in Tactile Afferents from the Fingers Eliciting Adaptive Motor Responses During Precision Grip," *Experimental Brain Research*, vol. 66, pp. 141–154, 1987.
- [5] V. G. Macefield, C. Häger-Ross, and R. S. Johansson, "Control of Grip Force During Restraint of an Object Held Between Finger and Thumb: Responses of Cutaneous Afferents from the Digits," *Experimental Brain Research*, vol. 108, pp. 155–171, 1996.
- [6] M. A. Srinivasan, J. M. Whitehouse, and R. H. LaMotte, "Tactile Detection of Slip: Surface Microgeometry and Peripheral Neural Codes," *Journal of Neurophysiology*, vol. 63, no. 6, pp. 1323–1332, 1990.
- [7] G. D. Lamb, "Tactile Discrimination of Textured Surfaces: Psychophysical Performance Measurements in Humans," *Journal of Physiology*, vol. 338, pp. 551–565, 1983.
- [8] M. Hollins, S. J. Bensmaïa, and S. Washburn, "Vibrotactile Adaptation Impairs Discrimination of Fine, but not Coarse, Textures," *Somatosensory & Motor Research*, vol. 18, no. 4, pp. 253–262, 2001.
- [9] S. Bensmaïa and M. Hollins, "Pacian Representations of Fine Surface Texture," *Perception & Psychophysics*, vol. 67, no. 5, pp. 842–854, 2005.
- [10] R. S. Johansson and G. Westling, "Roles of Glabrous Skin Receptors and Sensorimotor Memory in Automatic Control of Precision Grip when Lifting Rougher or More Slippery Objects," *Experimental Brain Research*, vol. 56, pp. 550–564, 1984.
- [11] H. R. Nicholls and M. H. Lee, "A Survey of Robot Tactile Sensing Technology," *International Journal of Robotics Research*, vol. 8, no. 3, pp. 3–30, 1989.
- [12] R. D. Howe, "Tactile Sensing and Control of Robotic Manipulation," *Advanced Robotics*, vol. 8, no. 3, pp. 245–261, 1994.
- [13] M. H. Lee and H. R. Nicholls, "Tactile Sensing for Mechatronics - A State of the Art Survey," *Mechatronics*, vol. 9, pp. 1–31, 1999.
- [14] R. S. Dahiya, G. Metta, M. Valle, and G. Sandini, "Tactile Sensing—From Humans to Humanoids," *IEEE Transactions on Robotics*, vol. 26, no. 1, pp. 1–20, 2010.
- [15] L. A. Jones and S. J. Lederman, *Human Hand Function*. Oxford University Press, USA, 2006.
- [16] R. D. Howe and M. R. Cutkosky, "Sensing Skin Acceleration for Slip and Texture Perception," in *IEEE International Conference on Robotics and Automation*, 1989, pp. 145–150.
- [17] P. Dario, D. de Rossi, C. Domenici, and R. Francesconi, "Ferroelectric Polymer Tactile Sensors with Anthropomorphic Features," in *IEEE International Conference on Robotics and Automation*, 1984, pp. 332–340.
- [18] J. S. Son, E. A. Monteverde, and R. D. Howe, "A Tactile Sensor for Localizing Transient Events in Manipulation," in *IEEE International Conference on Robotics and Automation*, 1994, pp. 471–476.
- [19] Y. Yamada and M. R. Cutkosky, "Tactile Sensor with 3-Axis Force and Vibration Sensing Functions and Its Application to Detect Rotational Slip," *IEEE International Conference on Robotics and Automation*, pp. 3550–3557, 1994.
- [20] P. Dario, M. Rucci, C. Guadagnini, and C. Laschi, "An Investigation on a Robot System for Disassembly Automation," in *Proceedings of IEEE International Conference on Robotics and Automation*, 1994, vol. 4, pp. 3515–3521.
- [21] J. Vranish, "Magnetoinductive skin for robots," in *IEEE International Conference on Robotics and Automation*, 1986, vol. 3, pp. 1292–1318.
- [22] B. Hutchings and A. Grahn, "Multiple-Layer Cross-Field Ultrasonic Tactile Sensor," in *IEEE International Conference on Robotics and Automation*, 1994, pp. 2522–2528.
- [23] S. Ando and H. Shinoda, "Ultrasonic Emission Tactile Sensing," *IEEE Control Systems*, vol. 15, pp. 61–69, 1995.
- [24] N. Wettels and G. E. Loeb, "Haptic Feature Extraction from a Biomimetic Tactile Sensor: Force, Contact Location and Curvature," in *IEEE International Conference on Robotics and Biomimetics*, 2011.
- [25] N. Wettels, L. M. Smith, V. J. Santos, and G. E. Loeb, "Deformable Skin Design to Enhance Response of a Biomimetic Tactile Sensor," in *IEEE/RAS-EMBS International Conference on Biomedical Robotics and Biomechanics*, 2008, pp. 132–137.
- [26] N. Wettels, V. J. Santos, R. S. Johansson, and G. E. Loeb, "Biomimetic Tactile Sensor Array," *Advanced Robotics*, vol. 22, no. 7, pp. 829–849, 2008.
- [27] J. A. Fishel, V. J. Santos, and G. E. Loeb, "A Robust Micro-Vibration Sensor for Biomimetic Fingertips," in *IEEE/RAS-EMBS International Conference on Biomedical Robotics and Biomechanics*, 2008, pp. 659–663.
- [28] C. H. Lin, T. W. Erickson, J. A. Fishel, N. Wettels, and G. E. Loeb, "Signal Processing and Fabrication of a Biomimetic Tactile Sensor Array with Thermal, Force and Microvibration Modalities," in *IEEE International Conference on Robotics and Biomimetics*, 2009, pp. 129–134.
- [29] R. S. Johansson, U. Landstrom, and R. Lundstrom, "Responses of Mechanoreceptive Afferent Units in the Glabrous Skin of the Human Hand to Sinusoidal Skin Displacements," *Brain Research*, vol. 244, no. 1, pp. 17–25, 1982.
- [30] H.-Y. Yao and V. Hayward, "Design and Analysis of a Recoil-Type Vibrotactile Transducer," *Journal of Acoustical Society of America*, vol. 128, no. 2, pp. 619–627, 2010.